Volume 1 | Number 1 | Jan 2013 | Pages 1–100

Journal of
Materials Chemistry C

Materials for optical and electronic devices
www.rsc.org/materialsC

ROYAL SOCIETY
OF CHEMISTRY

This is an *Accepted Manuscript*, which has been through the Royal Society of Chemistry peer review process and has been accepted for publication.

Accepted Manuscripts are published online shortly after acceptance, before technical editing, formatting and proof reading. Using this free service, authors can make their results available to the community, in citable form, before we publish the edited article. We will replace this *Accepted Manuscript* with the edited and formatted *Advance Article* as soon as it is available.

You can find more information about *Accepted Manuscripts* in the **Information for Authors**.

ROYAL SOCIETY
OF CHEMISTRY

www.rsc.org/materialsC

Synthesis and Properties of Air-Stable n-Channel Semiconductors Based on MEH-PPV Derivatives Containing Benzo[*c*]cinnoline Moieties

Jyh-Chien Chen,*[a] Hsin-Chung Wu,[a] Chi-Jui Chiang,[a] Tuo Chen,[a] Li Xing[b]

[a] Department of Materials Science and Engineering, National Taiwan University of Science and Technology, No. 43 Sec. 4 Keelung Road, Taipei, 10607, Taiwan

[b] Pfizer Worldwide Research and Development, 200 Cambridge Park Drive, Cambridge, MA 02140, USA

Corresponding Author: Jyh-Chien Chen

Department of Materials Science and Engineering, National Taiwan University of Science and Technology, No. 43 Sec. 4 Keelung Rd., Taipei, 106, Taiwan

Tel.: +886-2-27376526

Fax: +886-2-27376544

E-mail: jcchen@mail.ntust.edu.tw

ABSTRACT:

In this study we synthesized three novel poly[2-methoxy-5-(2-ethylhexyloxy)-1,4-phenylenevinylene] (MEH-PPV) derivatives that differ in terms of their ratios of heterocyclic benzo[c]cinnoline moieties: **P50** containing only MEH-PPV/benzo[c]cinnolinevinylene (BZCV) alternating segments and **P25** and **P10** containing both MEH-PPV/BZCV alternating segments and MEH-PPV block segments. UV-Vis and PL spectra of these polymers revealed values of λ_{max}^{UV} and λ_{max}^{PL} that ranged from 440 to 489 and from 492 to 551 nm, respectively; these wavelengths blue-shifted upon incorporating additional benzo[c]cinnoline moieties. We also observed energy transfer from the MEH-PPV/BZCV alternating segments to the MEH-PPV block segments. **P50**, which featured an alternating structure in its main chain, displayed a solvatochromic effect, emitting green light in non-polar solvents and yellow light in polar solvents. The HOMO and LUMO energy levels of these polymers, measured using cyclic voltammetry, ranged from -5.11 to -5.62 and from -3.08 to -3.31 eV, respectively. The incorporation of electron-withdrawing benzo[c]cinnoline moieties enhanced the electron affinity and improved the oxidative stability of the polymers. A bottom-gate, top-contact organic field-effect transistor (OFET) based on **P50** exhibited n-channel behavior under ambient conditions, with an electron mobility of 7.8×10^{-3} cm^{2}V^{-1}s^{-1} and an on/off ratio greater than 10^4. No significant variation in electron mobility can be observed after this OEFT was stored under ambient conditions up to 30 days. To the best of our knowledge, this is the first time that air-stable n-channel MEH-PPV derivatives have ever been reported. It indicated that p-type MEH-PPV can be transformed into n-type materials upon incorporation of benzo[c]cinnoline moieties.

transistor

INTRODUCTION

Organic conjugated polymers exhibit unique optoelectronic properties that make them applicable in organic light-emitting diodes (OLEDs), organic photovoltaic cells (OPCs), and organic field-effect transistors (OFETs).[1-11] Unlike traditional inorganic materials, the structures of organic conjugated polymers are readily tunable for various purposes through chemical reactions. They also offer attractive advantages such as flexibility, light weight, inexpensive preparation, and solution-processability. Since the first report in 1986 of a p-channel OFET based on a polythiophene film grown electrochemically,[11, 12] impressive advances have been made in enhancing the hole mobility through developments in both chemical structures and fabrication techniques. Several materials exhibit hole mobility of greater than 1 $cm^2V^{-1}S^{-1}$,[13-17] with some even exceeding 8 $cm^2V^{-1}S^{-1}$.[17] Although progress has also been made in the development of n-type electron-transporting conjugated polymers to enhance the performance of n-channel OFETs,[4-11, 18] air-stable n-type conjugated polymers exhibiting high electron mobility remain rare. In most cases, their electron mobility must be measured in a dry box.

Poly[2-methoxy-5-(2-ethylhexyloxy)-1,4-phenylenevinylene] (MEH-PPV) is a p-type conjugated polymer possessing a low ionization potential. Electron-withdrawing groups have been incorporated into the backbones or side chains of MEH-PPVs with the goal of enhancing the electron affinity, the electron injection/transporting ability, and corresponding OLED performance.[19-24] In addition, intra- or intermolecular charge transfer, energy transfer, lower-lying energy levels for highest occupied molecular orbitals (HOMO) and lowest unoccupied molecular orbitals (LUMO), and changes in emissive colors have also been observed for various MEH-PPV derivatives.[19-24] The hole mobility of MEH-PPVs has been

investigated using various methods, including the space-charge limited current (SCLC), the time of flight (TOF), and OFETs.[25-30] OFETs based on pristine MEH-PPV can exhibit ambipolar properties under a N_2 atmosphere when the MEH-PPV has been annealed, a crosslinked polymer has been used as the dielectric, and calcium has been used as the contact electrodes.[31] Nevertheless, several following examples of OFETs based on electron-rich MEH-PPVs, or MEH-PPV derivatives containing electron-withdrawing 1,3,4-oxadiazole moieties, have exhibited only p-channel characteristics, with hole mobility in the range from 10^{-4} to 10^{-5} $cm^2V^{-1}S^{-1}$.[32, 33] To the best of our knowledge, no MEH-PPV based OFETs have ever been reported to exhibit n-type characteristics under ambient conditions.

Benzo[c]cinnoline and its derivatives are planar, nitrogen-containing heterocyclic compounds that can be physiologically active.[34] The synthesis of benzo[c]cinnoline typically involves reductive cyclization of 2,2'-dinitrobiphenyls.[35] Their optical properties are sensitive to solvent environments. For example, enhanced photoluminescence quantum yields and phosphorescence have been observed in alcoholic solvents.[36-38] It has also been calculated that benzo[c]cinnoline moieties can lower HOMO and LUMO energy levels more effectively than phenanthrene moieties.[39] From a previous study of the electrochemical properties of poly(1,3,4-oxadiazole)s, we reported that benzo[c]cinnoline can indeed lower the HOMO and LUMO energy levels of conjugated polymers.[40]

In this present study, we used the Horner-Wadsworth-Emmons reaction to synthesize the MEH-PPV derivatives **P50**, **P25**, and **P10**, which differ in terms of the ratios of benzo[c]cinnolinevinylene (BZCV) moieties. We recorded UV-Vis and photoluminescence spectra of these polymers to investigate the energy transfer between the MEH-PPV block segments and the MEH-PPV/BZCV alternating segments. We also employed solvents of different dielectric constants to examine solvatochromism. We measured, through cyclic voltammetry, the effect of introducing the electron-withdrawing benzo[c]cinnoline moieties

on the polymers' HOMO and LUMO energy levels. Finally, to investigate the effects of the benzo[c]cinnoline moieties on the carrier mobility, we fabricated OFETs and measured their performance.

EXPERIMENTAL

Materials

4,4'-Dibromo-2,2'-dinitrobiphenyl (**1**), 3,8-dibromobenzo[c]cinnoline (**2**), 3,8-dicyanobenzo[c]cinnoline (**3**) were synthesized according to our previous report.[40] 2-Methoxy-5-(2-ethylhexyloxy)-1,4-phenyldialdehyde (**5**) and 2-methoxy-5-(2-ethylhexyloxy)-1,4-bis(diethoxyphosphinyl-methyl)-benzene (**6**) were prepared following literature procedures.[41, 42] Tetrabutylammonium perchlorate (TBAP) used in cyclic voltammetric measurements was recrystallized twice with ethyl acetate and dried at 120 °C under reduced pressure overnight. The other reagents were purchased from commercial companies and used as received. All of the solvents used in this study were purified according to standard methods prior to use.

Measurements

Melting points were determined on a Mel-Temp capillary melting point apparatus. Proton (^{1}H NMR) and carbon (^{13}C NMR) nuclear magnetic resonance spectra were recorded at 500 and 125 MHz, respectively, on a Bruker Avance-500 spectrometer. Infrared spectra were obtained with a Digilab-FTS1000 FTIR. Mass spectroscopy was conducted using a Finnigan TSQ 700 mass spectrometer. Molecular weights were measured on a JASCO gel permeation chromatography (GPC) system (PU-980) equipped with an RI detector (RI-930) and a Jordi Gel DVB mixed bed column (250 mm × 10 mm), using dimethylacetamide (DMAc) as the eluent, and calibrated with polystyrene standards. Thermal gravimetric analyses (TGA) were

performed in nitrogen with a TA TGA Q500 thermogravimetric analyzer operated at a heating

rate of 10 °C min^{-1}. Differential scanning calorimetry (DSC) was conducted under a N_2

atmosphere using a PerkinElmer DSC 4000 analyzer operated at a heating rate of 20 °C/min.

UV-Vis spectroscopy was performed using a JASCO V-670 UV-Vis/NIR spectrophotometer.

Photoluminescence (PL) was measured using a JASCO FP-8500 spectrofluorometer. The PL

quantum yields (Φ_{PL}) of the polymers in tetrahydrofuran (THF) were measured using 10^{-5} M

quinine sulfate in 1 N H_2SO_4 as the reference standard ($\Phi_{PL} = 0.546$). Cyclic voltammetry

(CV) was conducted at room temperature using a CH Instrument 611C electrochemical

analyzer and a three-electrode electrochemical cell comprising a working electrode (polymer

film coated on ITO glass), a reference electrode [Ag/Ag$^+$, referenced against

ferrocene/ferrocenium (Fc/Fc$^+$), 0.09 V], and a counter electrode (Pt gauze)-operated at a

scan rate of 100 mV s^{-1}. CV of polymer films was performed using an electrolyte solution of

0.1 M tetrabutylammonium perchlorate (TBAP) in MeCN. The potential windows for the

oxidative and reductive scans were from 0 to +2.0 and from 0 to -2.0 V, respectively.

Synthesis of Monomer

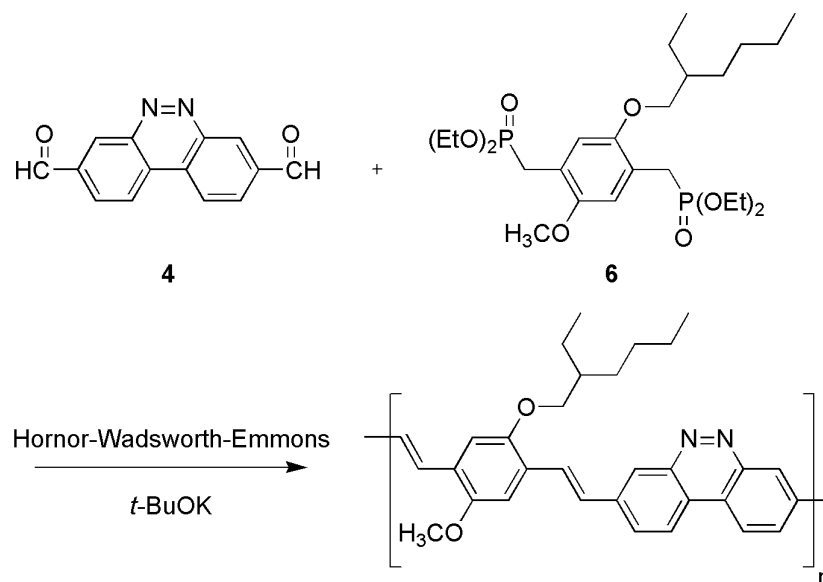**3,8-Dicarbaldehydebenzo[c]cinnoline (4)**
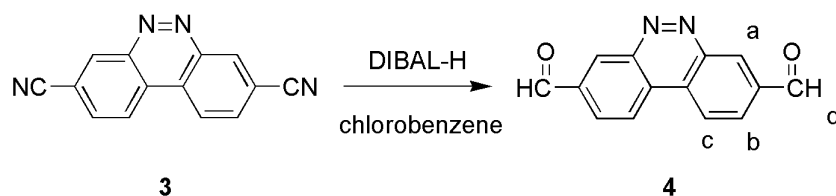
To a 250-mL, three-necked, round-bottomed flask equipped with a condenser was added

3,8-dicyanobenzo[c]cinnoline (**3**) (1.00 g, 4.35 mmol) in chlorobenzene (150 mL) under

nitrogen atmosphere. After 9 mL (10.09 mmol) of diisobutylaluminium hydride (DIBAL-H)

(20% in hexane) was slowly added with a syringe, the reaction mixture was further stirred at

0 °C overnight. The reaction mixture was poured into a vigorously stirred 300 mL solution of

methanol/water (1:1, v/v) with ice bath for 30 min. After 100 mL of 3.0 M HCl solution was

added and stirred for 10 min, the reaction mixture was extracted with ethyl acetate. The

combined organic phase was washed with water, dried over anhydrous $MgSO_4$. After the

solvent was evaporated, the collected solid was purified by column chromatography using

ethyl acetate/chloroform (2:8) as the eluent to afford 0.22 g (yield: 22%) of yellow powder.

mp > 275 °C (decompose). ^1H NMR (500 MHz, DMSO-d_6, δ, ppm): 10.41 (s, 2H,

aldehyde-H_d) 9.34 (d, J = 1.5 Hz, 2H, Ar-H_a), 9.17 (d, J = 8.5 Hz, 2H, Ar-H_c), 8.49 (dd, J_1 =

8.5 Hz, J_2 = 1.5 Hz, 2H, Ar-H_b). ^{13}C NMR (125 MHz, DMSO-d_6, δ, ppm): 192.54, 145.00,

137.54, 134.55, 129.50, 124.63, 123.80. Anal. Calcd: C, 71.18; H, 3.41; N, 11.86. Found: C,

70.65; H, 3.66; N, 11.51. EIMS (m/z): calcd. for $C_{14}H_8N_2O_2$, 236.1; found, 236.1 [M^+].

Synthesis of Polymers

P50

To a 50-mL, three-neck, round-bottom flask were added

3,8-dicarbaldehydebenzo[c]cinnoline **4** (0.2361 g, 1.0 mmol), 2-methoxy-5-(2-ethylhexyloxy)

-1,4-bis(diethoxyphosphinyl-methyl)-benzene **6** (0.5363 g, 1.0 mmol), and 40 mL of dry

DMF. 1.0 M *t*-BuOK (6 mL, 6.0 mmol, in THF solution) was slowly added with a syringe under nitrogen atmosphere. The mixture was stirred at room temperature for 48 h under N_2 before being poured into water. The precipitate was filtered off, washed with hot MeOH (Soxhlet apparatus) for 12 h, and then dried at 100 °C overnight under reduced pressure to afford a deep-red solid 0.2118 g (yield: 43%).

P25

Feed Ratio of **4**:**5**:**6** = **P25**: 0.5:0.5:1
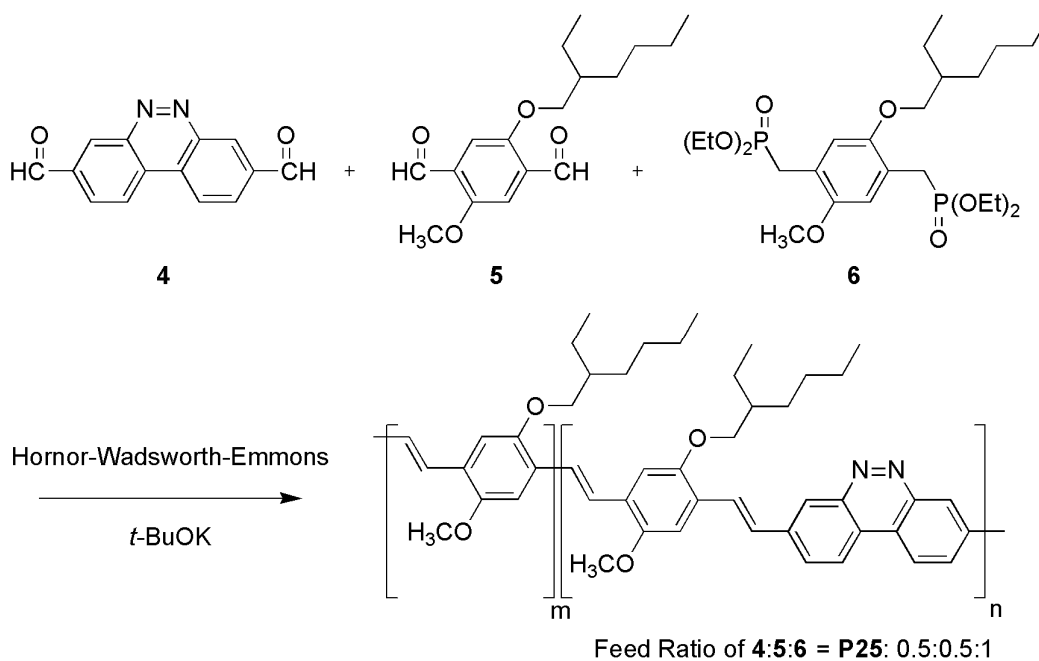
The polymer was synthesized following the same procedure as **P50** with compound **4** (0.1180 g, 0.5 mmol), compound **5** (0.1461 g, 0.5 mmol), and compound **6** (0.5363 g, 1.0 mmol) to afford a red solid 0.2291 g (yield: 44%).

P10

Feed Ratio of **4**:**5**:**6** = **P10**: 0.2:0.8:1
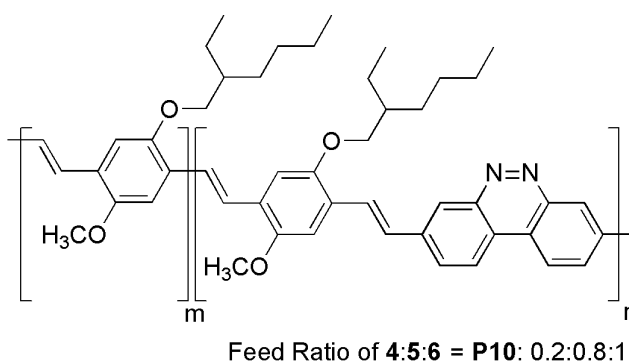
The polymer was synthesized following the same procedure as **P50** with compound **4** (0.0472 g, 0.2 mmol), compound **5** (0.2337 g, 0.8 mmol), and compound **6** (0.5363 g, 1.0 mmol) to afford a red solid 0.3440 g (yield: 64%).

Fabrication of Organic Field-Effect Transistors

OFET devices were fabricated with a bottom-gate, top-contact configuration. A heavily doped n^+-Si/SiO$_2$ wafer was used as the substrate, wherein the n^+-Si and thermally grown SiO$_2$ functioned as the gate electrode and dielectric, respectively. The wafer was washed sequentially with acetone and isopropanol. The SiO$_2$ dielectric surface was treated with a monolayer of *n*-octadecyltrichlorosilane (OTS) prior to spin-coating to prevent electron-trapping by the OH groups. An anhydrous solution of **P50** (1 mg/mL) in *N*-methyl-2-pyrrolidinone (NMP) was spin-coated (1000 rpm, 40 s) onto the modified SiO$_2$/n^+-Si substrate at room temperature and then the sample was dried on a hot plate under N$_2$ in a glove box to afford a thin film of **P50** (ca. 50 nm). The drain and source electrodes were deposited by thermally evaporating gold (Au) through a shadow mask. The channel width (*W*) and length (*L*) were 2000 and 50 μm, respectively. An OFET device based on MEH-PPV was also fabricated for comparison.

RESULTS AND DISCUSSION

Synthesis of Monomer

We prepared the monomer 3,8-dicarbaldehydebenzo[*c*]cinnoline (**4**) through a four-step synthesis (Scheme 1). 4,4'-Dibromo-2,2'-dinitrobiphenyl (**1**) was prepared from 2,5-dibromonitrobenzene through an Ullmann coupling reaction; it was then reduced by LiAlH$_4$ to form heterocyclic 3,8-dibromobenzo[*c*]cinnoline (**2**). We obtained 3,8-dicarbaldehydebenzo[*c*]cinnoline (**4**) after converting the bromo groups of **2** to cyano

groups[40] and then reducing them in the presence of DIBAL-H. Fig. S1 in supporting information displays the ^{1}H NMR spectrum of **4**. The signal at 10.41 ppm indicates that the cyano groups had been successfully converted into aldehyde groups. The ^{1}H NMR spectrum combined with the results from mass spectroscopy and element analysis confirms the formation of highly pure 3,8-dicarbaldehydebenzo[*c*]cinnoline (**4**). Compounds containing dialdehyde groups might be utilized for polymerization of conjugated polymers containing carbon-carbon double bond or carbon-nitrogen double bond linkages. In this research, a series of polymers containing carbon-carbon double bond linkages were synthesized by Hornor-Wadsworth-Emmons reaction.
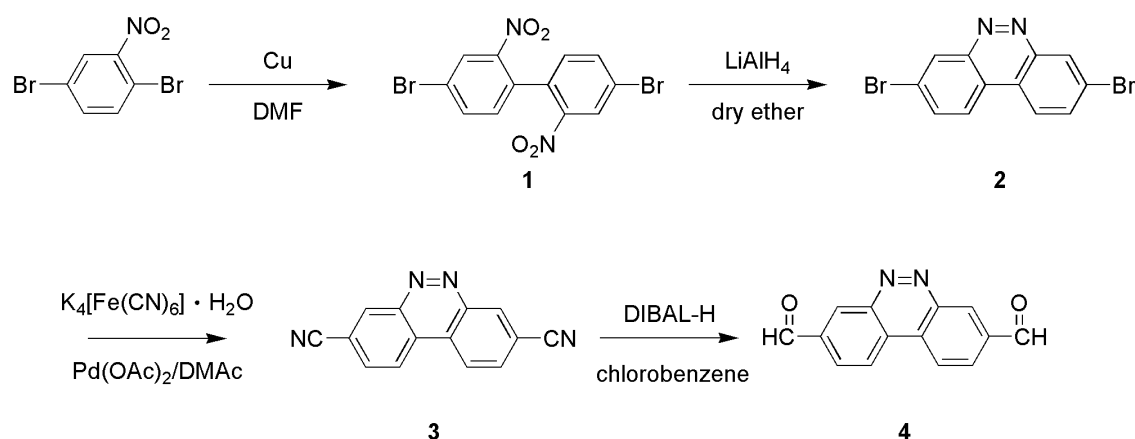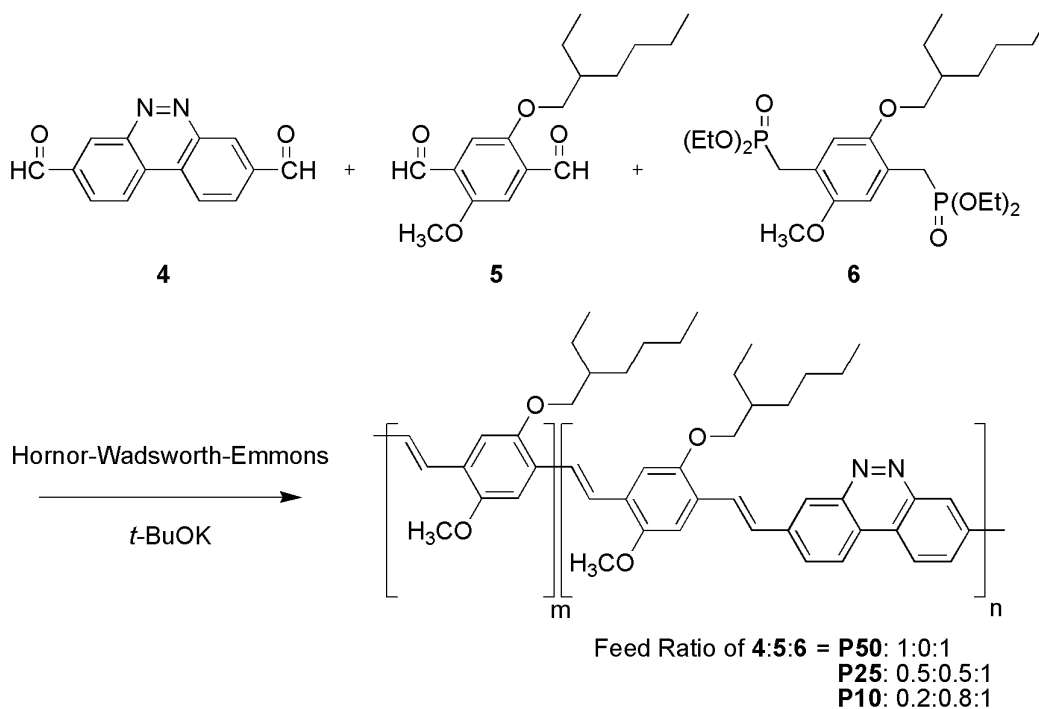

Scheme 1 Synthetic route of 3,8-dicarbaldehydebenzo[*c*]cinnoline (**4**).

Synthesis of Polymers

Scheme 2 presents our approach for the synthesis of the conjugated polymers **P50**, **P25**, and **P10** through Horner-Wadsworth-Emmons reactions of compounds **4**, **5**, and **6** in ratios of 1:0:1, 0.5:0.5:1, and 0.2:0.8:1, respectively. The number-average molecular weights (M_n) of **P50**, **P25**, and **P10** were all greater than 14,000 g/mol, as measured through GPC using DMAc as the eluent (Table 1). These conjugated polymers contain both

2-methoxy-5-(2-ethylhexyloxy)-1,4-phenylvinylene (MEH-PPV) and benzo[*c*]cinnolinevinylene (BZCV) segments. Based on the monomer feed ratios, **P50** is a complete alternating polymer of MEH-PPV and BZCV segments, while **P25** and **P10** contain both MEH-PPV/BZCV alternating segments and MEH-PPV block segments.

Assuming that all of the monomers were consumed, the theoretical ratios of the BZCV and MEH-PPV segments in **P25** and **P10** should be 25:75 and 10:90, respectively. The actual contents of BZCV segments in the main chains of **P25** and **P10**, determined using elemental analysis, were, however, 20 and 6%, respectively, presumably because of the low yields (43-64%) of these polymerization processes. This finding also suggests that the reactivity of 3,8-dicarbaldehydebenzo[*c*]cinnoline (**4**) is lower than that of 2-methoxy-5-(2-ethylhexyloxy)-1,4-phenyldialdehyde (**5**). The ^{1}H and ^{13}C NMR spectra of **P10** were shown in supporting information (Fig. S2 and S3). Although we did not observe (DSC) a glass transition for **P50** at temperatures of up to 350 °C, **P25** and **P10** underwent glass transitions at 148 and 117 °C, respectively. These polymers also exhibited good thermal stability, with the decomposition temperatures at 5% weight loss (T_d) all higher than 340 °C (Table 1). In the chosen solvents [NMP, DMF, DMAc, 1,2-dichlorobenzene (DCB), chloroform (CF), and THF], we determined the qualitative solubilities (Table 2) using 0.001 g of polymer in 1 mL of the solvent. **P50** was soluble upon heating in NMP, but only partially soluble in other tested solvents. **P10** was soluble in all solvents. The polymers became less soluble upon increasing the content of BZCV, presumably because the planarity and rigidity of the benzo[*c*]cinnoline moieties induced closer interchain packing and stronger intermolecular interactions.

4 **5** **6**

Hornor-Wadsworth-Emmons

t-BuOK

Feed Ratio of **4**:**5**:**6** = **P50**: 1:0:1
P25: 0.5:0.5:1
P10: 0.2:0.8:1

Scheme 2 Synthetic route of polymers.

Table 1 Molecular Weights and Thermal Properties of Polymers

Polymer	$M_n{}^a$	PDI[a]	Yield (%)	BZCV (%)[b] actual	BZCV (%)[c] theoretical	T_d (°C)[d]	T_g (°C)[e]	Char yield (wt%)[f]
P50	54000	1.51	43	50	50	372	-[g]	57
P25	14000	1.64	44	20	25	363	148	32
P10	30000	1.98	64	6	10	348	117	20

[a] Obtained from GPC using DMAc as solvent and calibrated with polystyrene standards.
[b] Actual percentage of BZCV, calculated by elemental analysis.
[c] Theoretical percentage of BZCV, calculated from feed ratio.
[d] Measured by TGA at a heating rate of 10 °C /min in nitrogen.
[e] Measured by DSC at a heating rate of 20 °C /min in nitrogen.
[f] Residual weight percentage at 800 °C in nitrogen.
[g] Not observed.

Table 2 Solubility of Polymers

Polymer	Solvent[a]					
	NMP	DMAc	DMF	DCB	CF	THF
P50	+	±	±	±	±	±
P25	++	++	+	±	±	±
P10	++	++	++	++	++	++

Abbreviations: NMP, *N*-methyl-2-pyrrolidinone; DMF, dimethylformamide; DMAc, dimethylacetamide; DCB, 1,2-dichlorobenzene; CF, chloroform; THF, tetrahydrofuran.
[a] Qualitative solubility was determined using 0.001 g of polymer in 1 mL of solvent. ++ (soluble at room temperature) ; + (soluble on heating at 60 °C) ; ± (partially soluble on heating at 60 °C).

Optical Properties

Fig. 1 (a) presents UV-Vis and PL spectra of **P50**, **P25**, **P10**, and MEH-PPV (each 10^{-5} M in THF); Table 3 summarizes the data. The maximum absorption wavelengths (λ_{max}^{UV}) appeared in the range from 440 to 489 nm, with the emission peaks (λ_{max}^{PL}) ranging from 492 to 551 nm. The shoulders evident in the PL spectra indicate the vibronic features of these polymers.[43-45] The absorption wavelengths and emission peaks underwent blue-shifting upon increasing the content of BZCV segments in the conjugated copolymers. The maximum absorption (λ_{max}^{UV}) and emission (λ_{max}^{PL}) of the **P50** solution (in THF) appeared at 440 and 492 nm, respectively. Because **P50** is a completely alternating conjugated polymer, consisting of MEH-PPV and BZCV segments, we can consider these two peaks as indicators of the absorptions and emissions from the MEH-PPV/BZCV alternating segments. On the other hand, we consider those peaks (absorption at 497 nm, emission at 554 nm) for the pristine MEH-PPV polymer to be indicators of the presence of the MEH-PPV block segments. We also characterized the polymers in terms of their optical properties in the solid state [Fig. 1 (b), Table 3]. The absorption edges had red-shifted to 700 nm or beyond, relative to those of the solution samples. Thus, the effective conjugation lengths of the polymers in the form of their solid films were longer than those in solution. The emission peaks were also red-shifted to within the range from 584 to 604 nm.

Conjugated polymers with donor-acceptor systems often exhibit red-shifted absorption wavelengths and lower band gaps as a result of intramolecular (or intermolecular) charge transfer (ICT) between their electron-withdrawing and electron-donating moieties.[2] ICT is an important effect that can be used to harvest more light energy and generate excitons more efficiently in photovoltaic applications. Although this effect can be related to planarity in main chain or to the formation of quinoid structures,[46] such behavior is not always observed in every donor-acceptor conjugated system. In this present study, for example, we could not detect any donor-acceptor ICT effect. Incorporating electron-withdrawing BZCV moieties into MEH-PPV did not lead to red-shifted absorption wavelengths nor lower band gaps. Likewise, the ICT effect was not observed either in other MEH-PPV systems containing various electron-withdrawing moieties.[19, 20, 22, 24, 47] It is possible that MEH-PPV segments are not appropriate donors for the ICT effect. In addition, because most donor-acceptor conjugated polymers contain thiophene moieties (or their derivatives) as their donors, it is the thiophene-acceptor-thiophene structures that generate charge transfer most effectively.[48-52] In some cases, the absorption edge can extend into the near-infrared region.[50-52] We hypothesize that polymerization of electron-withdrawing benzo[c]cinnoline (BZC) moieties with thiophene derivatives, or the synthesis of thiophene-BZC-thiophene structures, might induce ICT effects; accordingly, we are currently investigating the development of BZC-containing thiophene-based conjugated polymers for photovoltaic applications.

Table 3 Optical Properties of Polymers

Polymer	Solution (nm)[a]				Film		
	λ_{max}^{UV}	λ_{max}^{PL}	FWHM	Φ_{PL}^{b} (%)	λ_{max}^{UV}	λ_{onset}^{UV}	λ_{max}^{PL}
P50	440	492	72	23	428	550	584
P25	476	549	59	18	469	610	604
P10	489	551	40	18	510	610	604
MEH-PPV	497	554	40	25	511	600	600

[a] Measured in THF at a concentration of 10^{-5} M.
[b] Estimated using quinine sulfate (dissolved in 1 N $H_2SO_{4(aq)}$, assuming a value of Φ_{PL} of 0.546) as the standard.
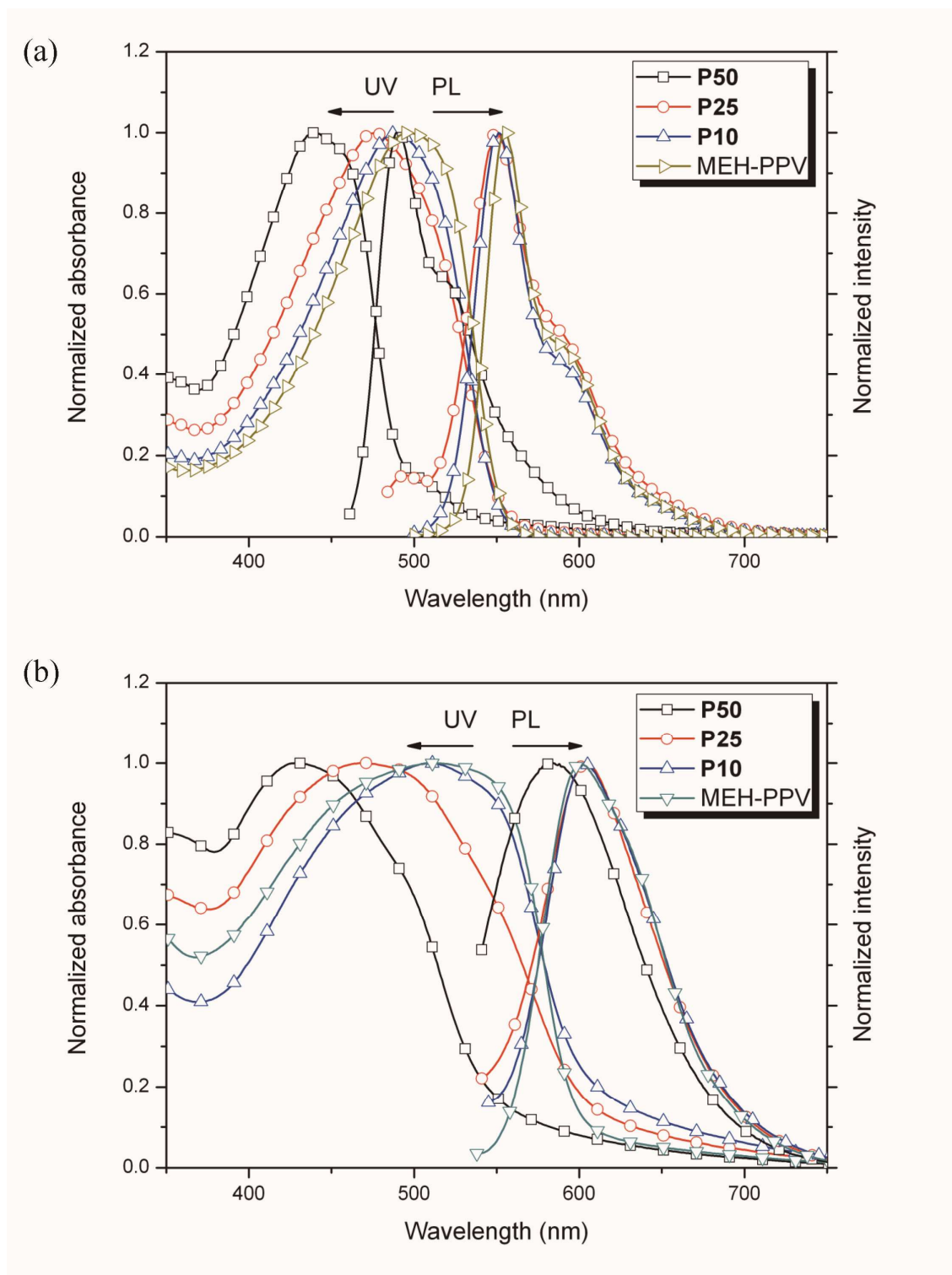
Fig. 1 UV-Vis absorption and PL emission spectra (upon excitation by λ_{max}^{UV} radiation) of the tested polymers (a) in THF at 10^{-5} M and (b) in the solid state.

It has been investigated that conjugated polymers with two different segments showed dual emissions from these two segments separately.[53, 54] Fig. 1 (a) reveals that **P25** exhibited two emission peaks at 549 and 500 nm. From a comparison with the emission peaks of pristine MEH-PPV and **P50**, we attribute these two emissions as arising from the MEH-PPV block segments (549 nm) and the MEH-PPV/BZCV alternating segments (500 nm). In addition, we observe spectral overlap between the absorption of the MEH-PPV and the emission of **P50**. It is speculated that the emissive energy from the MEH-PPV/BZCV alternating segments might be transferred to the MEH-PPV block segments.[55, 56] Thus, we used light at the value of λ_{max}^{UV} of **P50** (440 nm) to excite **P25** and **P10** in THF; Fig. 2 (a) reveals a major emission peak at 549 nm and a shoulder at 490 nm. We suspect that the emission peak at 549 nm, which we attribute to the emission of the MEH-PPV block segments, resulted from the MEH-PPV block segments directly absorbing the excitation radiation at 440 nm. It is also possible that the MEH-PPV block segments received the energy transferred from the emission of the MEH-PPV/BZCV alternating segments, because of the overlap between the emission peak of the MEH-PPV/BZCV alternating segments and the absorption peak of the MEH-PPV block segments. Fig. 2 (b) presents our proposed mechanism.[57]

The emission shoulder peak of **P25** at 490 nm in Fig. 2 (a) suggests incomplete energy transfer between the MEH-PPV/BZCV alternating segments and the MEH-PPV block segments. We attribute this behavior to the short lifetime of the exciton of the MEH-PPV/BZCV alternating segments, leading to extinction prior to absorption by the MEH-PPV block segments; it might also be possible that the extinction coefficient of the MEH-PPV block segments was too low to absorb the emission energy completely.

In the case of **P10**, we do not observe the emission shoulder at 490 nm in Fig. 2 (a), presumably because of the low concentration of the MEH-PPV/BZCV alternating segments relative to the MEH-PPV block segments.
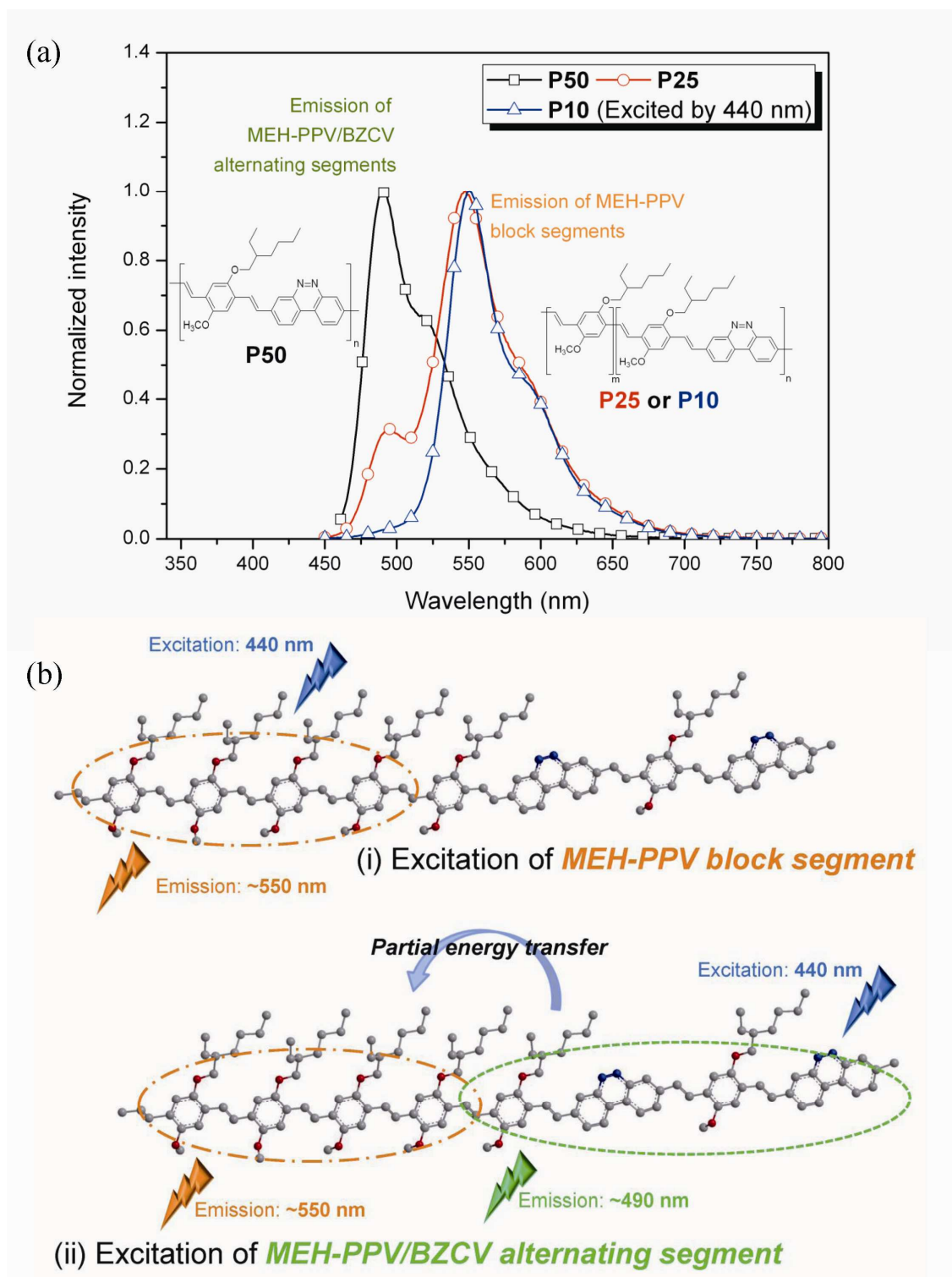
Fig. 2 (a) PL emission spectra of **P50**, **P25,** and **P10** in THF at 10^{-5} M excited by 440 nm radiation. (b) Proposed model of the excitation and emission mechanism with intramolecular

energy transfer between the MEH-PPV/BZCV alternating segments and the MEH-PPV block segments.

The optical properties of small molecules and polymers containing electron-donating and electron-withdrawing groups can be sensitive to the solvent polarity-that is, they display solvatochromism-as a result of intramolecular charge transfer.[24, 58-62] In this study, we investigated the solvatochromism of **P50**, which consists of an alternating structure, with the dielectric constants of the solvents used as an index of polarity. Fig. 3 (a) displays UV-Vis and PL spectra of **P50** in the non-polar solvents THF and DCB (dielectric constants: <15) and in the polar solvents DMAc and NMP (dielectric constants: >15). The absorption spectra of **P50** in these different solvents are similar, with no perceptible red-shifts of the peak maximum. In contrast, the PL emission spectra reveal not only red-shifted peaks but also the gradually broadening curves upon increasing the solvent polarity. In addition, Fig. 3 (b) reveals that **P50** in the different solvents emitted light of different colors after excitation at 365 nm: green in THF and DCB and yellow in DMAc and NMP. We attribute this positive fluorosolvatochromism to the higher dipole moment in the excited state than in the ground state, due to photoexcited charge transfer. Thus, the excited state would be stabilized more in polar solvents, leading to red-shifted peaks in the PL emission spectra.[63-67]

In general, molecules having larger dipole moments in the excited state than in the ground state also exhibit more red-shifted absorptions upon increasing the solvent polarity. In this study and in some other cases,[68] however, only the signals in the PL spectra were red-shifted. This phenomenon might be explained by differences in the times required for absorption, emission, and molecular reorientation in the solvents. The absorption of light by molecules occurs within a period of approximately 10^{-15} s. It takes approximately 10^{-10} s for solvents to reorient. Thus, no red-shift in absorption spectra would be observed if a solvent did not have

sufficient time to reorient. In contrast, the fluorescence lifetime typically ranges from 10^{-8} to 10^{-9} s-much longer than the time required for reorientation. Such molecules in the excited state will be exposed to the reoriented solvents and, therefore, the energy of the excited state will be lower as a result of stabilization provided by the reoriented solvents, leading to red-shifts in PL spectra.[68]
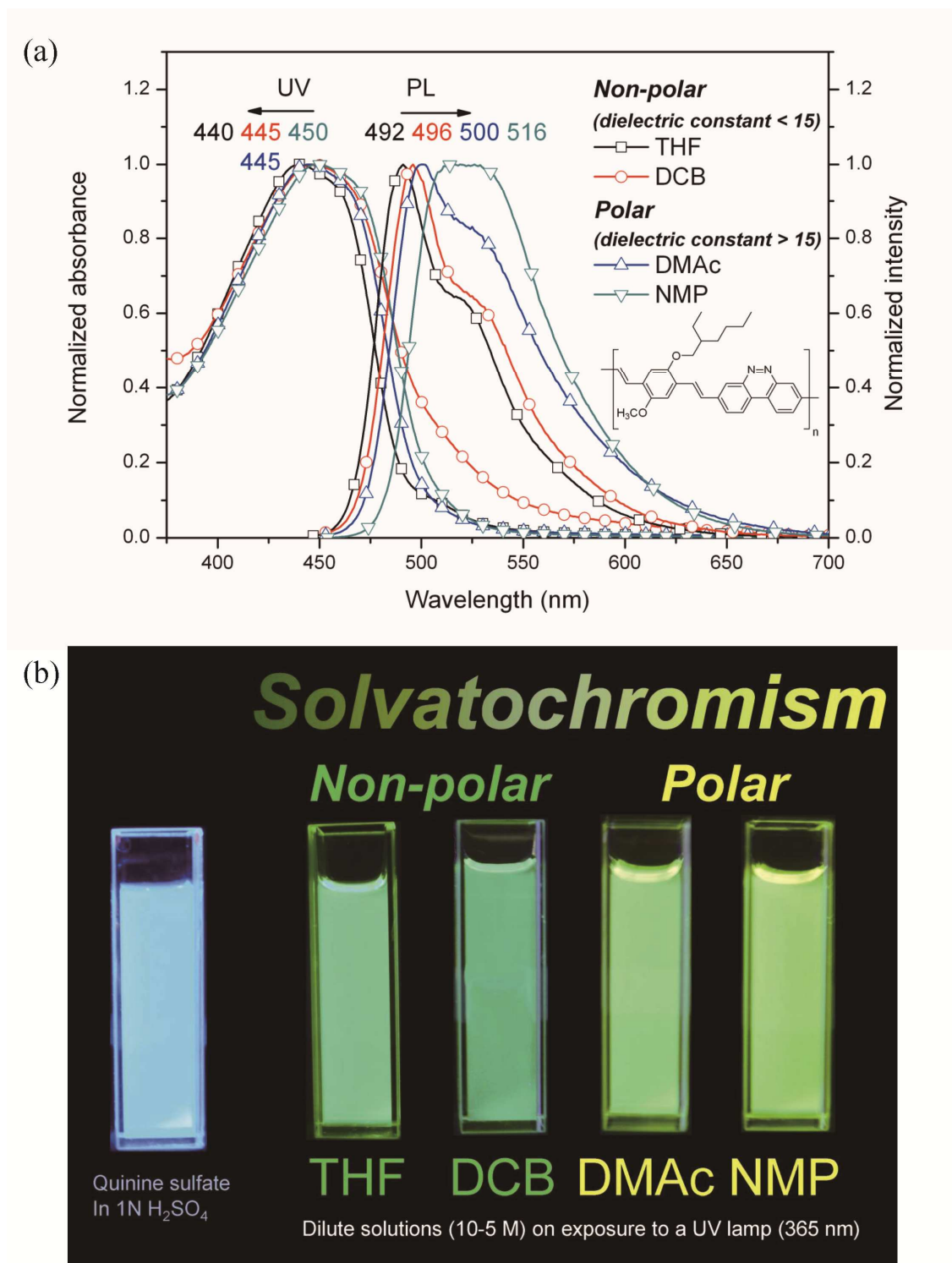
Fig. 3 (a) UV-Vis absorption and PL emission spectra of **P50** in THF, DCB, DMAc, and NMP at 10^{-5} M. (b) Colors emitted from dilute solutions of **P50** up exposure to light (365 nm) from a UV lamp.

To further investigate the solvatochromism of **P50** in polar solvents, we tested its behavior in mixed solvents of NMP and water at volume ratios from 5:1 to 1:1. We chose water for this study because it has a very high dielectric constant (80.1; thereby allowing tuning of the solvent polarity upon mixing with NMP) and because the optical properties of heterocyclic benzo[*c*]cinnoline rings are sensitive to solvents capable of hydrogen bonding[37, 38] (i.e., we suspected that hydrogen bonding between water and the benzo[*c*]cinnoline ring might also influence the optical properties of **P50**).

Table 4 lists the dielectric constants we calculated for mixed solvents containing NMP and water at various volume ratios. The absorption spectra of **P50** in these NMP/water mixtures changed only slightly, similar to the behavior displayed in Fig. 3 (a). Fig. 4 (a) presents PL spectra of **P50** in the various NMP/water mixtures; we observe red-shifting of λ_{max}^{PL} and peak broadening upon increasing the dielectric constant and water content of the mixed solvent. This effect might be also due to hydrogen bonding between the heterocyclic benzo[*c*]cinnoline and water. Accordingly, we tested another mixed solvent system-NMP and MeOH-to investigate the PL solvatochromism of **P50**. We chose MeOH because it has a dielectric constant (32.7) similar to that of NMP (31.7) while also allowing hydrogen bonding with the benzo[*c*]cinnoline moieties. Fig. 4 (b) displays PL spectra of **P50** in NMP/MeOH mixed solvents at volume ratios of 3:1 and 1:1. The values of λ_{max}^{PL} and the peak shapes in these PL spectra barely changed. Even though hydrogen bonding existed in the NMP/MeOH mixtures, the dielectric constants hardly changed at all. Thus, a comparison of Fig. 4 (a) and 4 (b) allows us to conclude that the PL solvatochromism of **P50** resulted only from the solvent polarity and was independent of hydrogen bonding.

Table 4 Optical Properties of **P50** in Different Solvents

Optical property	THF $(7.6)^a$	DCB $(9,9)$	DMAc (37.8)	NMP (31.7)	$5:1^b$ $(37.9)^c$	4:1 (39.23)	3:1 (41.24)	2:1 (44.74)	1:1 (52.31)
λ_{max}^{PL}	492	496	500	516	545	560	562	577	583
Φ_{PL}^{d} (%)	23.26	4.75	2.99	9.42	0.57	0.46	0.35	0.25	0.16

[a] Dielectric constant of the solvent.

[b] Volume ratio of NMP and water.

[c] Dielectric constant calculated using the equation: $\varepsilon_{mix}=[(\varepsilon_{NMP}^{1/3}-\varepsilon_{water}^{1/3})\Phi_{NMP}+\varepsilon_{water}^{1/3}]^3$, where ε_{NMP} and ε_{water} are the dielectric constants of NMP and water, respectively, and Φ_{NMP} is the volume fraction of NMP.[69]

[d] Estimated using quinine sulfate (dissolved in 1 N $H_2SO_{4(aq)}$, assuming a value of Φ_{PL} of 0.546) as the standard. Refractive indices of mixed solvents were calculated using the Lorentz-Lorenz equation.[70]
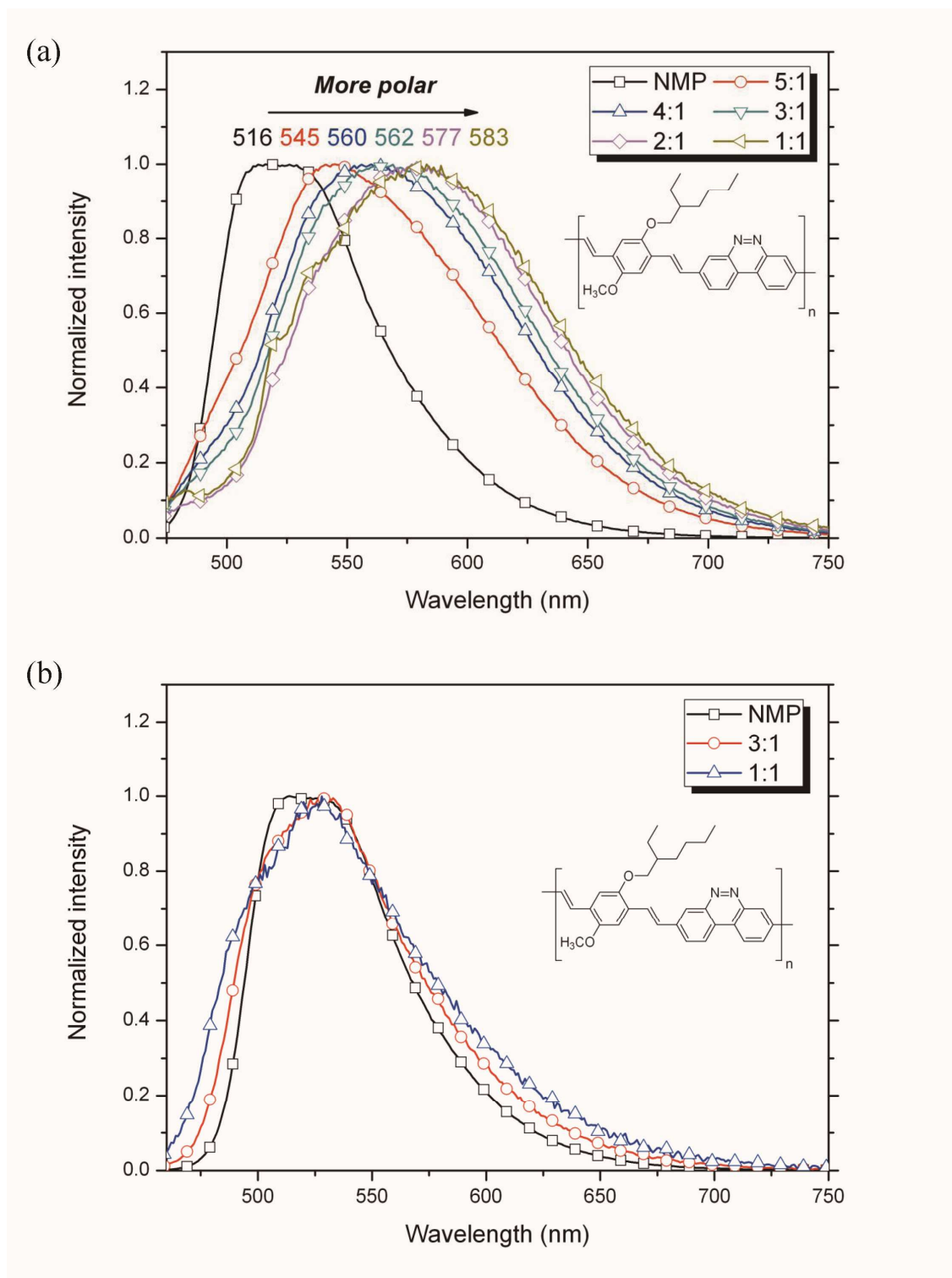
(a)

(b)

Fig. 4 (a) PL emission spectra of **P50** in NMP/H$_2$O (volume ratios: 5:1, 4:1, 3:1, 2:1, and 1:1) at 10^{-5} M. (b) PL emission spectra of **P50** in NMP/CH$_3$OH (volume ratios: 3:1 and 1:1) at 10^{-5} M.

Electrochemical Properties

We used CV to characterize the electrochemical redox behavior of our polymers. Fig. S4 presents cyclic voltammograms of **P50**, **P25**, and **P10** in the form of thin films. We observe irreversible anodic and cathodic scans for each polymer. The onset potentials for oxidation and reduction of these polymers ranged from 0.40 to 0.91 and from -1.4 to -1.63 eV, respectively. We calculated the HOMO [ionization potential (IP)] and LUMO [electron affinity (EA)] energy levels from the onset potentials of oxidation and reduction, respectively. The absolute energy level of ferrocene/ferrocenium (Fc/Fc$^+$) is assumed to be 4.8 eV below vacuum level. The external Fc/Fc$^+$ redox standard $E_{1/2}$ was determined to be 0.09V versus Ag/Ag$^+$ in acetonitrile by our electrochemical measuring system.[71] Table 5 summarizes the CV data. The calculated HOMO and LUMO energy levels of **P50**, **P25**, and **P10** ranged from -5.62 to -5.11 and from -3.31 to -3.08 eV, respectively. The energy band gaps calculated from these electrochemical measurements ranged from 1.94 to 2.31 eV. Among these polymers, **P50** had the lowest-lying HOMO and LUMO energy levels (-5.62 and -3.31 eV, respectively).

In a previous study,[40] we found that the nitrogen-containing heterocyclic benzo[c]cinnoline has good electron affinity; accordingly, the introduction of benzo[c]cinnoline moieties into conjugated polymers would lower their HOMO and LUMO energy levels. In this study, we found that **P50**, **P25**, and **P10** all had HOMO and LUMO energy levels (Table 5) lower than those of MEH-PPV (E_{HOMO} = -5.07 eV; E_{LUMO} = -2.90 eV).[72] In addition, their HOMO and LUMO energy levels were more low-lying upon increasing the content of benzo[c]cinnoline.

Table 5 Electrochemical Properties of Polymers

Polymer	E_{onset}^{ox} (V)[a]	E_{onset}^{red} (V)[a]	E_{HOMO} (eV)[b]	E_{LUMO} (eV)[c]	E_g^{ec} (eV)[d]	E_g^{opt} (eV)[e]
P50	0.91	-1.40	-5.62	-3.31	2.31	2.25
P25	0.52	-1.63	-5.23	-3.08	2.15	2.21
P10	0.40	-1.54	-5.11	-3.17	1.94	2.21
MEH-PPV[f]	-	-	-5.07	-2.90	2.17	2.21

[a] Measured by cyclic voltammetry.
[b] $E_{HOMO} = -(E_{onset}^{ox} + 4.80 - 0.09)$ (eV).
[c] $E_{LUMO} = -(E_{onset}^{red} + 4.80 - 0.09)$ (eV).
[d] $E_g^{ec} = IP(E_{onset}^{ox}) - EA(E_{onset}^{red})$ (eV).
[e] Calculated using the equation: $1240/\lambda_{onset}$.
[f] Ref. 72.

To provide further evidence for the observed electrochemical properties of these polymers, we performed theoretical calculations. The method was described in supporting information. Fig. 5 displays the calculated HOMO and LUMO contours of MEH-PPV and **P50**. For MEH-PPV, the HOMO and LUMO orbitals are localized mainly on the phenyl rings. For **P50**, the electron density of the HOMO is localized mainly on the phenylenevinylene segment, while that of the LUMO is localized mainly on the BZCV segment. The simulation suggests that the first electron added to **P50** is most likely received by the electron-withdrawing benzo[c]cinnoline moieties and adjacent vinylene bonds.
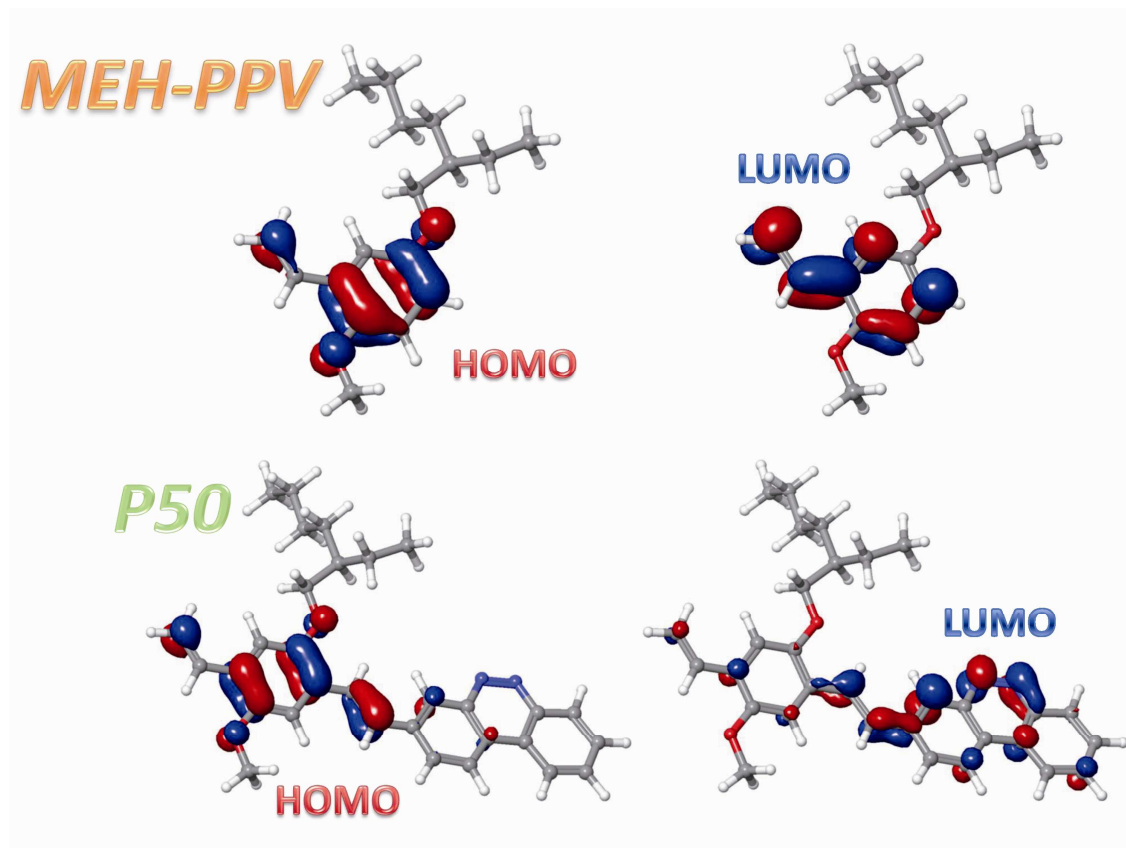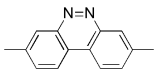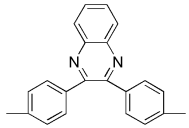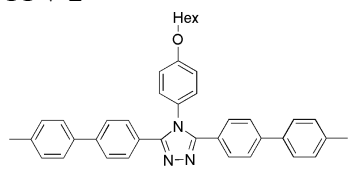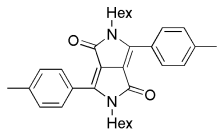
Fig. 5 Calculated HOMO and LUMO contours of MEH-PPV and **P50**.

Several nitrogen-containing heterocyclic moieties have also been incorporated into MEH-PPV to adjust the polymer's HOMO and LUMO energy levels. For example, MEH-PPV derivatives containing quinoxaline (PPV-1),[20] triazole (PPV-2),[47] and diketopyrrolopyrrole (PPV-3)[73] with alternating structure have been reported. Table 6 summarizes their electrochemical properties. The LUMO energy level of **P50** (E_{LUMO} = -3.31 eV) is comparable with those of PPV-2 (E_{LUMO} = -3.35. eV) and PPV-3 (E_{LUMO} = -3.36 eV), but lower than that of PPV-1 (E_{LUMO} = -2.63 eV). It indicates that the electron affinity of benzo[c]cinnoline is stronger than that of quinoxaline (PPV-1) and comparable with those of triazole (PPV-2) and diketopyrrolopyrrole (PPV-3). The HOMO energy level of **P50** (E_{HOMO} = -5.61 eV) is the lowest among these reported MEH-PPV derivatives containing nitrogen-containing heterocyclic rings. It suggests that **P50** would have good oxidative

stability.

Table 6 Electrochemical Properties of MEH-PPV Derivatives Containing Electron-Withdrawing Moieties

-Ar-	E_{onset}^{ox} (V)	E_{onset}^{red} (V)	E_{HOMO} (eV)	E_{LUMO} (eV)	E_g^{ec} (eV)	Ref.
	0.91	-1.40	-5.62	-3.31	2.31	This study
PPV-1	0.88	-1.77	-5.28	-2.63	2.65	20
PPV-2	0.32	-1.45	-5.12	-3.35	1.77	47
PPV-3	0.79	-1.18	-5.19	-3.36	1.94	73

Organic Field-Effect Transistor Performance

The carrier mobility of polymers was measured by OFET method. OFET devices based on **P50**, **P25**, **P10**, and MEH-PPV were fabricated in a bottom-gate, top-contact configuration using gold as the source and drain electrodes, and heavily doped n^+-Si as the gate electrode. Dielectric layer was OTS-treated SiO_2. The spin-coated polymer films were all annealing free. All of the OFET measurements were performed under ambient conditions. Fig. 6 displays the typical output and transfer characteristics of the OFET based on **P50**. We calculated the carrier mobility (μ) from the saturation regime in the transfer curves, according to the equation

$$I_{DS} = \mu(WC/2L)(V_G - V_T)^2$$

where W and L are the semiconductor channel width and channel length, respectively. C (17 nF/cm^2) is the capacitance of gate dielectric layer. V_T and V_G are the threshold and gate voltages, respectively. We determined the threshold voltage from the linear relationship between $I_{DS}^{1/2}$ versus V_G by extrapolating to $I_{DS} = 0$. Table 7 shows the carrier mobility, on/off ratios, and threshold voltages of MEH-PPV and its derivatives.

The OFET based on MEH-PPV, with the above-mentioned configuration, exhibited only p-channel characteristics, with a hole mobility (2.5 × 10^{-4} cm^{2}V^{-1}s^{-1}) on the same order as those reported in the literature.[27, 30] When the gate voltage was positive, the OFET based on MEH-PPV was inactive under ambient conditions, consistent with the p-type nature of MEH-PPV. The OFET based on **P10** only exhibited p-channel characteristic with hole mobility of 7.7 × 10^{-4} cm^{2}V^{-1}s^{-1}. In contrast, we could not determine the hole mobility of

P25 and **P50**. The OFETs of these two polymers only exhibited n-channel characteristics with electron mobility of 1.6 × 10^{-3} and 7.8 × 10^{-3} cm^{2}V^{-1}s^{-1}, threshold voltages of 12 and 10 V, respectively. Their on/off ratios were both greater than 10^4. These data were measured in air without annealing. These results indicate that p-type MEH-PPV can be transform into n-type materials by introducing an appropriate amount of electron-withdrawing benzo[c]cinnoline moieties on the main chain. This can be explained by the lower LUMO and HOMO energy levels resulted from the presence of the heterocycle. The lower LUMO energy level could facilitate electron injection, due to a lower energy barrier between the gold electrodes and the polymers, thereby facilitating electron mobility. In addition to enhanced air-stability, the lower HOMO energy level decreased the hole-transporting ability, such that **P25** and **P50** did not exhibit the characteristics of p-type materials.

Table 7 Performance of OFET Based on Polymers[a]

Polymer	μ_h (cm^{2}V^{-1}s^{-1})	μ_e (cm^{2}V^{-1}s^{-1})	I_{on}/I_{off}	V_T(V)
P50	-[a]	7.8×10^{-3}	10^4	10
P25	-	1.6×10^{-3}	10^4	12
P10	7.7×10^{-4}	-	10^4	-5
MEH -PPV	2.5×10^{-4}	-	10^4	-6

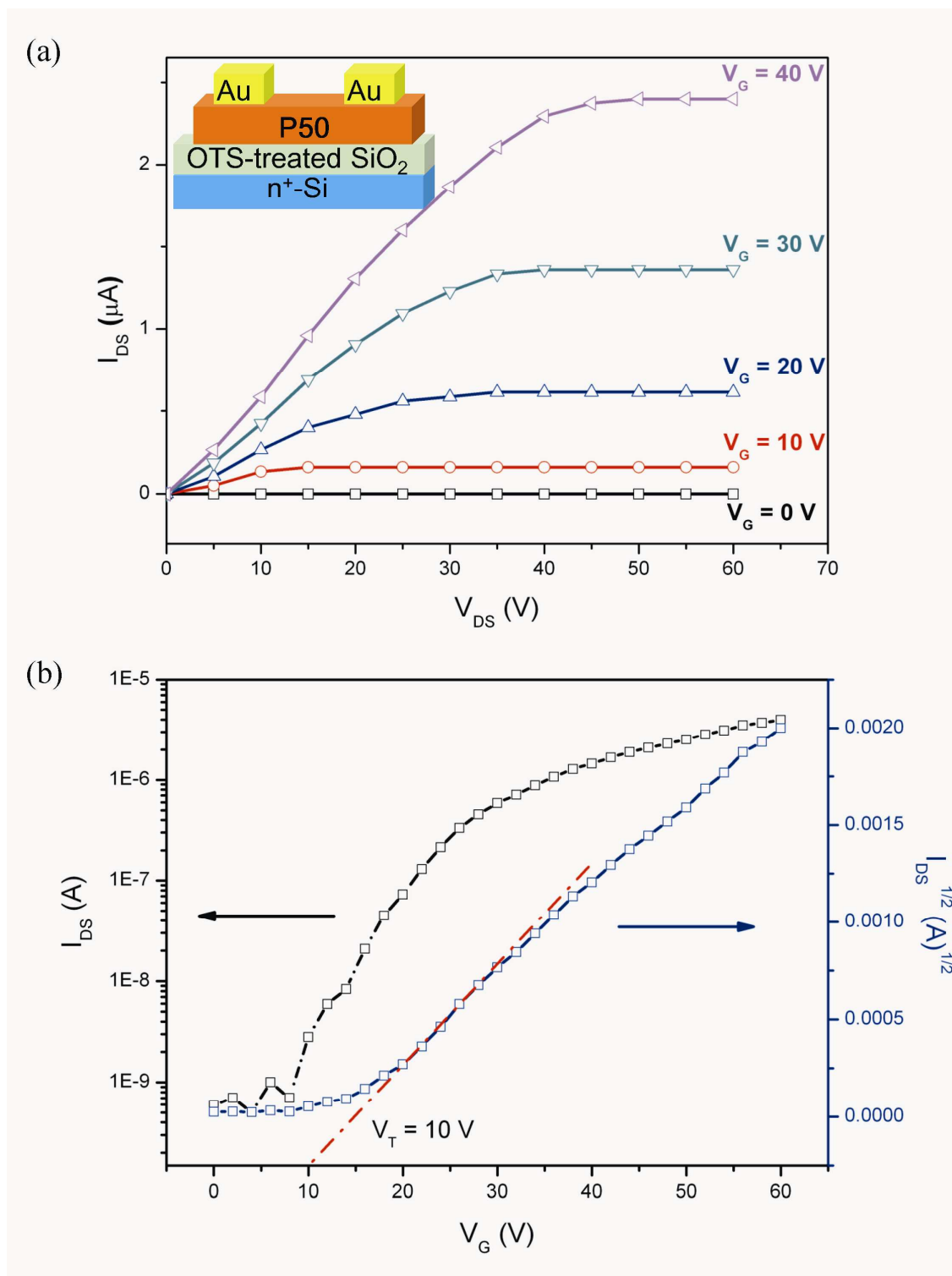[a] Measured under ambient conditions.
[b] Not available.

Fig. 6 Characteristics of an OFET based on **P50**, measured in air. (a) Output curves for various gate voltages; (b) transfer curves measured at a value of $V_{DS} = 30$ V.

In most cases, n-type OFETs reported previously have displayed complete inactivity in air or when prepared without annealing.[4, 74, 75] To the best of our knowledge, this paper reports the first example of OFET devices based on n-channel MEH-PPV derivatives that functions under ambient conditions. The electron mobility measured in air without annealing (1.6~7.8 $\times$ 10^{-3} $cm^2V^{-1}s^{-1}$) is at least two orders of magnitude higher than the only comparable value

(3 $\times$ 10^{-5} $cm^2V^{-1}s^{-1}$) reported in the literature, although that system used calcium electrodes, a crosslinked polymer as the dielectric, and was measured under a N_2 atmosphere.[31]

In order to further investigate the long-term air-stability, the performance of OFET based on **P50** was monitored during a 30-day period under ambient conditions. Fig. 7 shows the electron mobility on 10, 20, and 30 days after the device was fabricated. The electron mobility barely changes after 30 days from 7.8 $\times$ 10^{-3} to 6.5 $\times$ 10^{-3} $cm^2V^{-1}s^{-1}$, which are in the same order of magnitude without significant variation. It indicates that OFET based on **P50** can exhibit excellent air-stability.
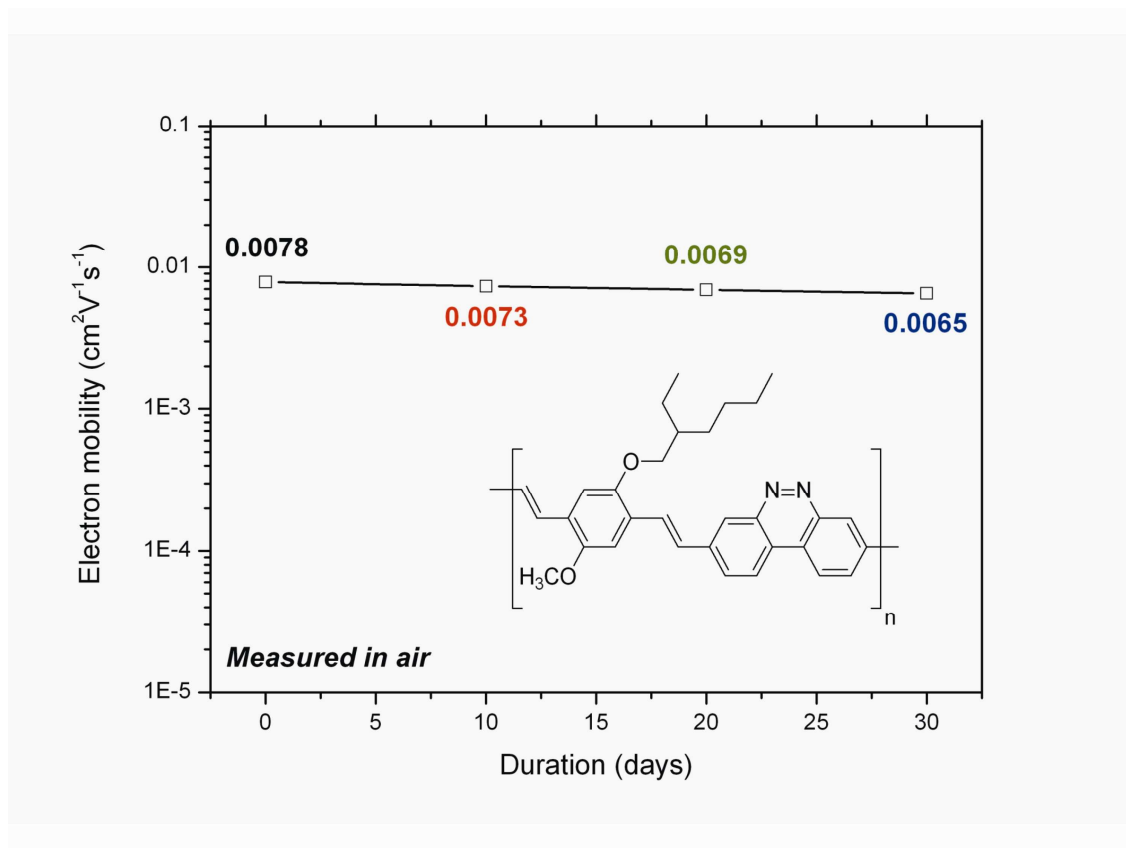
Fig. 7 Air-stability of OFET based on **P50**.

CONCLUSIONS

We have successfully synthesized MEH-PPV derivatives containing different amount of benzo[*c*]cinnolinevinylene (BZCV) segments on the main chain by Hornor-Wadsworth-Emmons reaction. These new conjugated polymers exhibited blue-shifts in their UV-Vis and PL spectra. **P50**, with completely alternating MEH-PPV/BZCV segments, exhibited PL solvatochromism that resulted solely from solvent polarity. The HOMO and LUMO energy levels were lower because the introduction of electron-withdrawing benzo[*c*]cinnoline moieties. We also demonstrate that p-type MEH-PPV can be transformed into n-type materials (**P25** and **P50)** when electron-withdrawing benzo[*c*]cinnoline moieties were introduced. The OFET electron mobility ($1.6 \sim 7.8 \times 10^{-3}$ $cm^{2}V^{-1}s^{-1}$) measured under

ambient conditions without annealing is two orders of magnitude higher than that of pristine MEH-PPV reported in the literature. The OFET based on **P50** also showed good air-stability up to 30 days. To the best of our knowledge, this is the first time that n-channel MEH-PPV derivatives with excellent air-stability have ever been reported.

REFERENCES AND NOTES

1.   L. Akcelrud, *Prog. Polym. Sci.*, 2003, 28, 875-962.

2.   C. L. Chochos and S. A. Choulis, *Prog. Polym. Sci.*, 2011, 36, 1326-1414.

3.   M.-C. Choi, Y. Kim and C.-S. Ha, *Prog. Polym. Sci.*, 2008, 33, 581-630.

4.   C. R. Newman, C. D. Frisbie, D. A. Da Silva Filho, J. L. Brédas, P. C. Ewbank and K. R. Mann, *Chem. Mater.*, 2004, 16, 4436-4451.

5.   J. Zaumseil and H. Sirringhaus, *Chem. Rev.*, 2007, 107, 1296-1323.

6.   A. R. Murphy and J. M. J. Fréchet, *Chem. Rev.*, 2007, 107, 1066-1096.

7.   A. Facchetti, *Mater. Today*, 2007, 10, 28-37.

8.   Y. Wen and Y. Liu, *Adv. Mater.*, 2010, 22, 1331-1345.

9.   J. E. Anthony, A. Facchetti, M. Heeney, S. R. Marder and X. Zhan, *Adv. Mater.*, 2010, 22, 3876-3892.

10.   X. Zhao and X. Zhan, *Chem. Soc. Rev.*, 2011, 40, 3728-3743.

11.   H. Usta, A. Facchetti and T. J. Marks, *Acc. Chem. Res.*, 2011, 44, 501-510.

12.   A. Tsumura, H. Koezuka and T. Ando, *Appl. Phys. Lett.*, 1986, 49, 1210-1212.

13.   W. Zhang, J. Smith, S. E. Watkins, R. Gysel, M. McGehee, A. Salleo, J. Kirkpatrick, S. Ashraf, T. Anthopoulos, M. Heeney and I. McCulloch, *J. Am. Chem. Soc.*, 2010, 132, 11437-11439.

14.   H. N. Tsao, D. M. Cho, I. Park, M. R. Hansen, A. Mavrinskiy, D. Y. Yoon, R. Graf, W. Pisula, H. W. Spiess and K. Müllen, *J. Am. Chem. Soc.*, 2011, 133, 2605-2612.

15.   J. S. Ha, K. H. Kim and D. H. Choi, *J. Am. Chem. Soc.*, 2011, 133, 10364-10367.

16.   J. Lee, A. R. Han, J. Kim, Y. Kim, J. H. Oh and C. Yang, *J. Am. Chem. Soc.*, 2012, 134, 20713-20721.

17.   H. Chen, Y. Guo, G. Yu, Y. Zhao, J. Zhang, D. Gao, H. Liu and Y. Liu, *Adv. Mater.*, 2012, 24, 4618-4622.

18.   M. Sommer, *J. Mater. Chem. C*, 2014, DOI: 10.1039/c3tc31755b.

19.   J. A. Mikroyannidis, I. K. Spiliopoulos, T. S. Kasimis, A. P. Kulkarni and S. A. Jenekhe, *J. Polym. Sci. Part A: Polym. Chem.*, 2004, 42, 2112-2123.

20.   P. Karastatiris, J. A. Mikroyannidis, I. K. Spiliopoulos, A. P. Kulkarni and S. A. Jenekhe, *Macromolecules*, 2004, 37, 7867-7878.

21.   B. C. Thompson, L. G. Madrigal, M. R. Pinto, T. S. Kang, K. S. Schanze and J. R. Reynolds, *J. Polym. Sci. Part A: Polym. Chem.*, 2005, 43, 1417-1431.

22.   W. F. Su, K. M. Yeh and Y. Chen, *J. Polym. Sci. Part A: Polym. Chem.*, 2007, 45, 4377-4388.

23.   L. Huo, Z. Tan, X. Wang, Y. Zhou, M. Han and Y. Li, *J. Polym. Sci. Part A: Polym. Chem.*, 2008, 46, 4038-4049.

24.   P. Karastatiris, J. A. Mikroyannidis and I. K. Spiliopoulos, *J. Polym. Sci. Part A: Polym. Chem.*, 2008, 46, 2367-2378.

25.   Y. Zhang, B. de Boer and P. W. M. Blom, *Phys. Rev. B*, 2010, 81, 085201.

26.   A. R. Inigo, C. H. Tan, W. Fann, Y. S. Huang, G. Y. Perng and S. A. Chen, *Adv. Mater.*, 2001, 13, 504-508.

27.   M. Muratsubaki, Y. Furukawa, T. Noguchi, T. Ohnishi, E. Fujiwara and H. Tada, *Chem. Lett.*, 2004, 33, 1480-1481.

28.   W. W. Zhu, S. Xiao and I. Shih, *Appl. Surf. Sci.*, 2004, 221, 358-363.

29.   Y. R. Liu, J. B. Peng and P. T. Lai, *Appl. Surf. Sci.*, 2007, 253, 6987-6991.

30. S.-i. Watanabe, H. Tanaka, S.-i. Kuroda, A. Toda, H. Tomikawa, S. Nagano and T. Seki, *Appl. Phys. Express*, 2012, 5, 021602.

31. L.-L. Chua, J. Zaumseil, J.-F. Chang, E. C.-W. Ou, P. K.-H. Ho, H. Sirringhaus and R. H. Friend, *Nature*, 2005, 434, 194-199.

32. H. Lee, D. Vak, K. J. Baeg, Y. C. Nah, D. Y. Kim and Y. Y. Noh, *J. Nanosci. Nanotechnol.*, 2013, **13**, 3321-3330.

33. C. A. Amorim, M. R. Cavallari, G. Santos, F. J. Fonseca, A. M. Andrade and S. Mergulhão, *J. Non-Cryst. Solids*, 2012, **358**, 484-491.

34. X. Shao, X. Luo, X. Hu and K. Wu, *J. Phys. Chem. B*, 2006, 110, 15393-15402.

35. O. V. Vinogradova and I. A. Balova, *Chem. Heterocycl. Compd.*, 2008, 1-22.

36. J. Waluk, A. Grabowska and B. Pakulstroka, *J. Lumin.*, 1980, 21, 277-291.

37. C. T. Lin and J. A. Stikeleather, *Chem. Phys. Lett.*, 1976, 38, 561-566.

38. H. Inoue, Y. Hiroshima and K. i. Tomiyama, *Bull. Chem. Soc. Jpn.*, 1981, 54, 2209-2210.

39. M. J. Sienkowska, J. M. Farrar, F. Zhang, S. Kusuma, P. A. Heiney and P. Kaszynski, *J. Mater. Chem.*, 2007, 17, 1399-1411.

40. J. C. Chen, H. C. Wu, C. J. Chiang, L. C. Peng, T. Chen, L. Xing and S. W. Liu, *Polymer*, 2011, 52, 6011-6019.

41. L. Huo, C. He, M. Han, E. Zhou and Y. Li, *J. Polym. Sci. Part A: Polym. Chem.*, 2007, 45, 3861-3871.

42. M. Kubo, C. Takimoto, Y. Minami, T. Uno, T. Itoh and M. Shoyama, *Macromolecules*, 2005, 38, 7314-7320.

43. G. Padmanaban and S. Ramakrishnan, *J. Am. Chem. Soc.*, 2000, 122, 2244-2251.

44. P. J. Lynch, L. O'Neill, D. Bradley, H. J. Byrne and M. McNamara, *Macromolecules*, 2007, 40, 7895-7901.

45. Y. Jin, J. Y. Kim, S. Song, Y. Xia, J. Kim, H. Y. Woo, K. Lee and H. Suh, *Polymer*, 2008, 49, 467-473.

46. H. A. M. van Mullekom, J. A. J. M. Vekemans, E. E. Havinga and E. W. Meijer, *Mater. Sci. Eng., R*, 2001, 32, 1–40.

47. S. H. Chen and Y. Chen, *Macromolecules*, 2005, 38, 53-60.

48. E. Wang, M. Wang, L. Wang, C. Duan, J. Zhang, W. Cai, C. He, H. Wu and Y. Cao, *Macromolecules*, 2009, 42, 4410-4415.

49. M. Zhang, X. Guo, X. Wang, H. Wang and Y. Li, *Chem. Mater.*, 2011, 23, 4264-4270.

50. E. Wang, L. Hou, Z. Wang, S. Hellström, F. Zhang, O. Inganäs and M. R. Andersson, *Adv. Mater.*, 2010, 22, 5240-5244.

51. H. Zhou, L. Yang, S. C. Price, K. J. Knight and W. You, *Angew. Chem. Int. Ed.*, 2010, 49, 7992-7995.

52. X. Guo, H. Xin, F. S. Kim, A. D. T. Liyanage, S. A. Jenekhe and M. D. Watson, *Macromolecules*, 2011, 44, 269-277.

53. F. B. Dias, S. Pollock, G. Hedley, L. O. Pålsson, A. Monkman, I. I. Perepichka, I. F. Perepichka, M. Tavasli and M. R. Bryce, *J. Phys. Chem. B*, 2006, 110, 19329-19339.

54. Q. Hou, Q. Zhou, Y. Zhang, W. Yang, R. Yang and Y. Cao, *Macromolecules*, 2004, 37, 6299-6305.

55. L. Zhang, S. Hu, J. Chen, Z. Chen, H. Wu, J. Peng and Y. Cao, *Adv. Funct. Mater.*, 2011, 21, 3760-3769.

56. S.-H. Chen and Y. Chen, *Macromolecules*, 2004, 38, 53-60.

57. J. Wakita, S. Inoue, N. Kawanishi and S. Ando, *Macromolecules*, 2010, 43, 3594-3605.

58. C. Reichardt, *Chem. Rev.*, 1994, 94, 2319-2358.

59. S. A. Jenekhe, L. Lu, M. M. Alam, *Macromolecules*, 2008, 34, 7315-7324.

60.   Q. Fang and T. Yamamoto, *Macromolecules*, 2004, 37, 5894-5899.

61.   J. Du, Q. Fang, X. Chen, S. Ren, A. Cao and B. Xu, *Polymer*, 2005, 46, 11927-11933.

62.   J. Natera, L. Otero, L. Sereno, F. Fungo, N.-S. Wang, Y.-M. Tsai, T.-Y. Hwu and K.-T. Wong, *Macromolecules*, 2007, 40, 4456-4463.

63.   Q. Fang, B. Xu, B. Jiang, H. Fu, X. Chen and A. Cao, *Chem. Commun.*, 2005, 1468-1470.

64.   W.-C. Wu, C.-L. Liu and W.-C. Chen, *Polymer*, 2006, 47, 527-538.

65.   G.-S. Liou, N.-K. Huang and Y.-L. Yang, *J. Polym. Sci. Part A: Polym. Chem.*, 2007, 45, 48-58.

66.   H. W. Chang, K. H. Lin, C. C. Chueh, G. S. Liou and W. C. Chen, *J. Polym. Sci. Part A: Polym. Chem.*, 2009, 47, 4037-4050.

67.   Y.-C. Kung, W.-F. Lee, S.-H. Hsiao and G.-S. Liou, *J. Polym. Sci. Part A: Polym. Chem.*, 2011, 49, 2210-2221.

68.   J. R. Lakowicz, *Principles of Fluorescence Spectroscopy*, Springer, Singapore, 3rd edn, 2006.

69.   K. L. Gering, L. L. Lee, L. H. Landis and J. L. Savidge, *Fluid Phase Equilib.*, 1989, 48, 111-139.

70.   M. S. Altuwaim, K. H. A. E. Alkhaldi, A. S. Al-Jimaz and A. A. Mohammad, *J. Chem. Thermodyn.*, 2012, 48, 39-47.

71.   T. Yasuda, T. Imase and T. Yamamoto, *Macromolecules*, 2005, 38, 7378-7385.

72.   Y. Li, Y. Cao, J. Gao, D. Wang, G. Yu and A. J. Heeger, *Synth. Met.*, 1999, 99, 243-248.

73.   G. Zhang, H. Xu, K. Liu, Y. Li, L. Yang and M. Yang, *Synth. Met.*, 2010, 160, 1945-1952.

74.   S. Zhang, Y. Wen, W. Zhou, Y. Guo, L. Ma, X. Zhao, Z. Zhao, S. Barlow, S. R.

Marder, Y. Liu and X. Zhan, *J. Polym. Sci. Part A: Polym. Chem.*, 2013, 51, 1550-1558.

75.   X. Zhao, Y. Wen, L. Ren, L. Ma, Y. Liu and X. Zhan, *J. Polym. Sci. Part A: Polym. Chem.*, 2012, 50, 4266-4271.

GRAPHICAL ABSTRACT
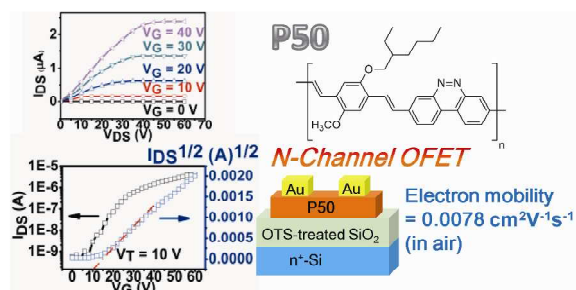
An OFET based on **P50** exhibited air-stable n-channel behavior with electron mobility of 7.8 $\times$ 10^{-3} cm^{2}V^{-1}s^{-1} under ambient conditions without annealing.